Regulated large-scale annual shutdown of Amazonian isoprene emissions?

Regulated large-scale annual shutdown of Amazonian isoprene emissions?

Michael P. Barkley,[1] Paul I. Palmer,[1] Isabelle De Smedt,[2] Thomas Karl,[3] Alex Guenther,[3] and Michel Van Roozendael[2]

Received 2 December 2008; accepted 7 January 2009; published 26 February 2009.

[1] We perform Empirical Orthogonal Function (EOF) analysis on 12 years of global GOME and SCIAMACHY formaldehyde (HCHO) column observations to determine the most significant spatial and temporal HCHO variations. In most regions, we find that HCHO variability is predominantly driven by seasonal variations of biogenic emissions and biomass burning. However, unusually low HCHO columns are consistently observed over the Amazon rainforest during the transition from the wet-to-dry seasons. We use MODIS leaf area and enhanced vegetation indices, to show variations in vegetation are consistent with the observed decrease in HCHO during this period (correlations of 0.69 and 0.67, respectively). Based on this evidence, we suggest isoprene emitting vegetation experience widespread leaf flushing (new leaf growth) prior to the dry season, resulting in a large-scale annual shutdown of Amazonian isoprene emissions. **Citation:** Barkley, M. P., P. I. Palmer, I. De Smedt, T. Karl, A. Guenther, and M. Van Roozendael (2009), Regulated large-scale annual shutdown of Amazonian isoprene emissions?, *Geophys. Res. Lett.*, *36*, L04803, doi:10.1029/2008GL036843.

1. Introduction

[2] Isoprene is a biogenic hydrocarbon that is emitted by terrestrial vegetation during the growing season largely as a function of temperature and light, the reasons for which are uncertain but are thought to improve plant tolerance against high temperatures and oxidants, or to serve as a carbon safety valve [*Guenther et al.*, 2006]. The climatic importance of this trace gas is due to it being a precursor for tropospheric ozone [*Sanderson et al.*, 2003] and organic aerosol [*Claeys et al.*, 2004], which affect air quality and the Earth's radiative balance. Current bottom-up models predict a global total of $\sim$500 Tg C a^{-1} [*Guenther et al.*, 2006], 70% emitted in the tropics, but the magnitude and distribution of these emissions are the subject of much speculation [*Arneth et al.*, 2008].

[3] Satellite observations of formaldehyde (HCHO), a high yield product of isoprene oxidation, provide additional constraints on surface isoprene emissions [*Palmer et al.*, 2003]. In the remote marine atmosphere the oxidation of methane provides a global HCHO background, but over land, significant enhancements in the boundary layer can occur from the oxidation of short-lived anthropogenic, pyrogenic and biogenic volatile organic compounds (VOCs), and through direct HCHO emissions from biomass burning, industrial processes and vegetation. Nadir sensors, e.g., GOME [*Burrows et al.*, 1999] and SCIAMACHY [*Bovensmann et al.*, 1999], which measure UV-spectra from which HCHO vertical columns can be retrieved, are sensitive to such enhancements allowing HCHO columns to act as a suitable proxy for mapping surface VOC emissions on spatial scales of order 100 km [*Palmer et al.*, 2003]. Several studies, using GOME HCHO data [*Chance et al.*, 2000], have shown that isoprene is the dominant VOC driving HCHO column variability, and have used this relationship to quantify isoprene emissions over North America [*Palmer et al.*, 2006], Asia [*Fu et al.*, 2007] and tropical South America [*Barkley et al.*, 2008] with an uncertainty of 40–100%.

[4] Recently, a continuous 12-year record of GOME and SCIAMACHY HCHO column measurements [*De Smedt et al.*, 2008] have become available allowing study of the year-to-year variability of HCHO. In this work we examine the variability in these HCHO global data using EOF analysis, and use meteorological and vegetation data to discuss the relationship with isoprene emissions and biomass burning. We present evidence that suggests a large-scale shutdown of Amazonian isoprene emissions during May–June, associated with the transition from the wet-to-dry seasons.

2. HCHO Column Retrievals From GOME and SCIAMACHY

[5] HCHO slant columns are retrieved from GOME and SCIAMACHY using UV absorption spectroscopy [*De Smedt et al.*, 2008]. The key difference, compared with previous studies [e.g., *Chance et al.*, 2000], is the choice of fitting window (328.5–346 nm) which minimizes fitting uncertainties due to a polarization anomaly affecting the SCIAMACHY spectra around 350 nm, and a major absorption band of the O_4 collision complex (centred near 360 nm). This choice of fitting window decreases fitting residuals within the Tropics, reduces noise over the oceans, and allows HCHO columns over desert regions (typically underestimated) to converge to background levels. To minimize errors created by spectral artifacts from GOME's diffuser plate [*Richter and Wagner*, 2001], a reference sector correction is applied, determined from daily GOME observations over the central Pacific Ocean (140°–160°W). Vertical columns are obtained by dividing the slant columns by an air mass factor (AMF) [*Palmer et al.*, 2001; *Martin et al.*, 2002], calculated using scattering weights computed by the radiative transfer model DISORT [*Kylling et al.*, 1995], and HCHO vertical profiles taken from the IMAGESv2 global chemistry transport model [*Müller and Stavrakou*,

[1]School of GeoSciences, University of Edinburgh, Edinburgh, UK.
[2]Belgian Institute for Space Aeronomy, Brussels, Belgium.
[3]National Center of Atmospheric Research, Boulder, Colorado, USA.

0094-8276/09/2008GL036843

2005]. Cloud fraction, albedo and top-height, used as input to DISORT, are provided by the FRESCO v5 algorithm [*Koelemeijer et al.*, 2002]. The total error on monthly averaged HCHO columns ranges from ~20%, within the Tropics, to 20–40% at higher latitudes (owing to greater spectral interference from ozone). In this study we assemble monthly mean HCHO distributions by averaging the data on to a 2° × 2.5° (latitude × longitude) grid, between 60°N–40°S, excluding columns with >40% cloud coverage. Use of a stricter cloud threshold has a negligible effect on our analysis.

3. HCHO Column Variability

3.1. Global Patterns

[6] To determine the most significant variations in the HCHO distributions, we perform EOF analysis on the monthly averaged fields (see auxiliary material).[1] To remove noise, which can introduce false patterns into the EOF modes, we smooth the monthly mean distributions with a 3 × 3 box-car filter and set grid squares over the South Atlantic Anomaly (which degrades the HCHO retrievals) to background values. Figure 1 shows the first 3 EOF modes explain a total of 51% of the total variance; higher modes show decreased contributions (<5%) to the total variance and it is difficult to assign physical meaning.

[7] The first EOF pattern, explaining 30% of the HCHO variability, has a principal component that oscillates in phase with the Earth's seasonal cycle, and is associated with increased biogenic emissions during (a) the growing season at northern mid-latitudes (June–September), and (b) the dry season within the Tropics (August–October). This feature is strongest over the US, tropical Africa and the Amazon. The HCHO columns over these regions are strongly correlated with temperature and direct photosynthetically active radiation (PAR) (Figure S1), which are the main drivers of isoprene emissions. Biogenic emissions coupled with seasonal agricultural burning on the North China Plain and forest fires in the Russian Far East, dominate the HCHO signal over east Asia [*Fu et al.*, 2007]. Biomass burning also contributes significantly to the HCHO columns in the Tropics; over the Amazon burning is more widespread in the dry season (August–December), but over Africa, a dipole pattern exists owing to different seasonal burning (and emissions) either side of the Equator (due to the migratory shift of the Inter-Tropical Convergence Zone; ITCZ).

[8] The second EOF mode, which explains 14% of the HCHO variability, is dominated by a strong feature over the Amazon which consistently shows a significant drop in the HCHO columns during the region's wet-to-dry transitional period (May–June) [*Trostdorf et al.*, 2004]. We discuss this feature in more detail in Section 4. Low HCHO columns are also periodically observed during these months over southwest Africa, before the onset of the region's burning season (July–December), and over Borneo.

[9] Biomass burning dominates the third EOF pattern, which comprises 8% of the HCHO variability. The principal component has a two maxima during each year owing to HCHO emitted from agricultural fires during (a) April–May over Central America, Venezuela and Columbia, and March over Southeast Asia, and (b) June–September over Indonesia and the Congo Basin.

3.2. HCHO Within the Tropics

[10] Interpreting HCHO variability over tropical regions is difficult owing to the complex coupling between biomass burning, biogenic emissions, and climate, which are influenced by the dynamics of the ITCZ, and events such as the El Niño Southern Oscillation (ENSO). Over the Amazon, isoprene oxidation and biomass burning are both significant HCHO sources [*Barkley et al.*, 2008], and separation of biogenic and pyrogenic contributions to the HCHO columns requires care. Figure S1 shows biomass burning is dominant over eastern Amazonia, reflected by Along Track Scanning Radiometer (ATSR) firecount data, but less so in western areas, where biogenic activity is easier to distinguish [*Barkley et al.*, 2008]. Only in northwest Amazonia, are HCHO columns significantly correlated with ENSO (Figure S1), most likely due to increased isoprene emissions [*Müller et al.*, 2008] associated with warmer and sunnier conditions [*Malhi and Wright*, 2004].

[11] In contrast, over Indonesia we find that biomass burning is the dominant source of HCHO, as temporal correlations with ATSR firecount data over Borneo and Sumatera are 0.89 and 0.75, respectively (Figure S2). The effect of ENSO is also more strongly felt here than elsewhere (Figure S1), with extremely high HCHO columns ($>2.0 \times 10^{16}$ molecules cm^{-2}) detected over Borneo during the intense El Niño event of 1997/98, a consequence of large forest and peat fires.

[12] Over tropical Africa, HCHO variability is linked to the movement of the ITCZ, and ENSO has little effect (Figure S1). Using ATSR firecount data (Figure S2), we find that from the Gold Coast across to the Central African Republic, burning peaks in January (when the ITCZ is typically southernmost), with the HCHO reaching a maximum in March–April. In contrast, over the Congo Basin, the main burning period peaks in July (when the ITCZ is northernmost) with the HCHO peaking in August–September. Increased cloud cover, associated with the ITCZ, is also likely to inhibit biogenic VOC emissions owing to cooler temperature and lower light levels.

4. Large-Scale Shutdown of Amazonian Isoprene Emissions?

[13] The second EOF mode revealed a significant drop in HCHO columns over the Amazon during the wet-to-dry transitional period (Figure 1). Here we focus on a sub-region of the Amazon rainforest (Figure S3) and isolate biogenic contributions to the HCHO columns by removing scenes influenced by surface fires, identified using measurements of firecounts and concurrent NO_2 column measurements $>0.8 \times 10^{15}$ molecules cm^{-2} [*Barkley et al.*, 2008]. To determine the monthly mean time series of HCHO over the Amazon we average the pre-screened grid squares falling within our study domain. Over this region, model studies and in situ measurements show isoprene is the dominant biogenic VOC; emissions of monoterpenes and methylbutenol are likely to be a least an order of magnitude smaller [*Barkley et al.*, 2008, and references therein].

[1] Auxiliary materials are available in the HTML. doi:10.1029/2008GL036843.

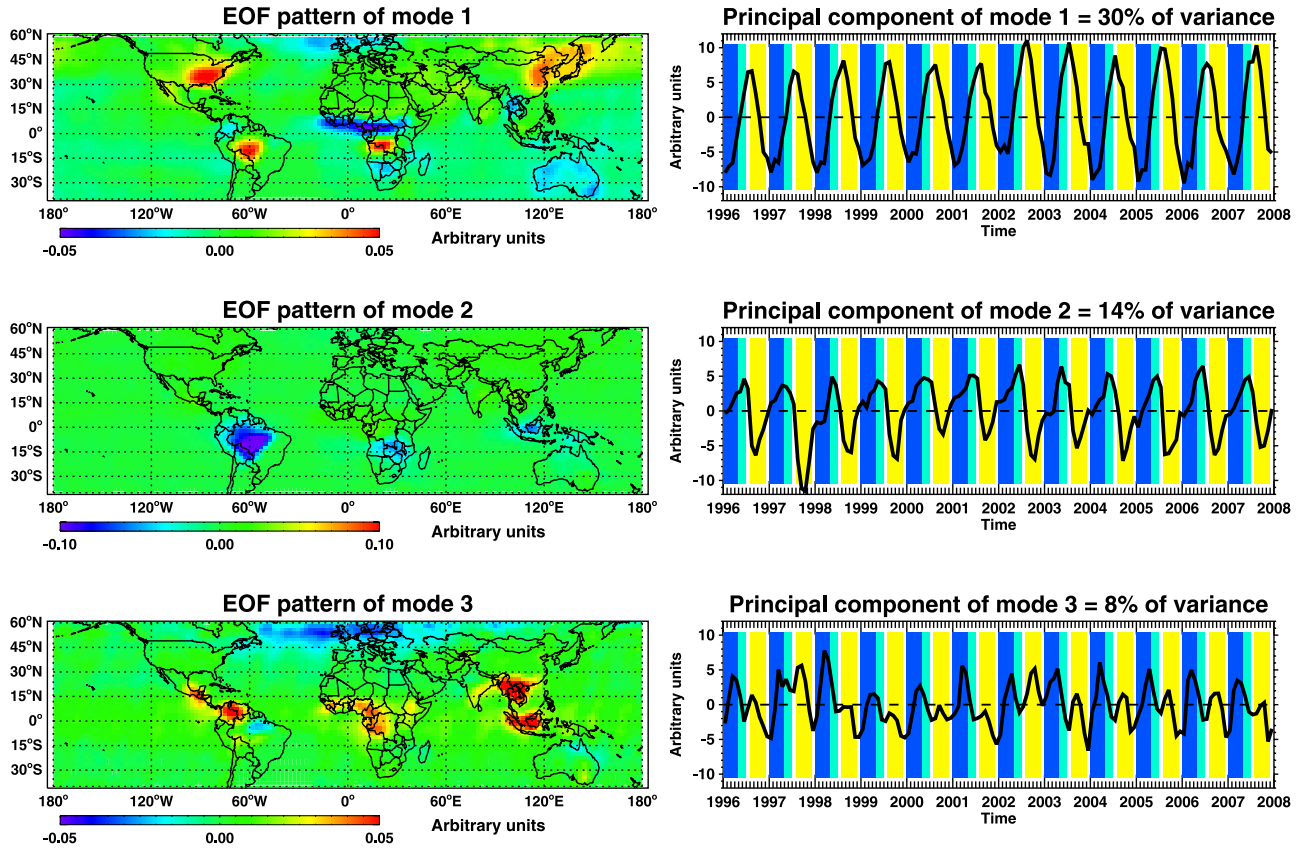

Figure 1. The first three eigenvectors of the Empirical Orthogonal Function (EOF) analysis of the monthly HCHO column distributions averaged on to 2° × 2.5° (latitude × longitude) grid, excluding scenes with >40% cloud coverage. The (left) EOF regression maps and (right) principal components with their corresponding eigenvalues show the dominant spatial and temporal variations of the HCHO columns, respectively. The dark blue, light blue, and yellow regions shown on the principal components represent the wet (January–April), transition (May–June), and dry (August–November) seasons over the Amazon [*Barkley et al.*, 2008], respectively.

[14] Figure 2a shows there is a largely unexplained HCHO seasonal cycle over the Amazon basin [*Trostdorf et al.*, 2004], recurring year-to-year over 1997–2007, which is qualitatively consistent with sparse in situ concentration data over this region [*Kesselmeier et al.*, 2002], but which chemistry-transport models generally have difficulty in reproducing [*Barkley et al.*, 2008]. Seasonal variations of isoprene are consistent with HCHO, with wet season concentrations (January–April) typically 20–40% lower than those in the dry season (August–December) (Figures 2b and 2c). HCHO columns during the wet-dry transition period are much lower than in the wet or dry seasons and are close to background values [*Barkley et al.*, 2008]. This implies that isoprene fluxes are close to zero over this transition period or that concentrations of the hydroxyl radical, the principal sink of isoprene and HCHO, are unexpectedly low. The dry-to-wet period does not show a similar dramatic reduction. Recent top-down emission estimates over western Amazonia [*Barkley et al.*, 2008], showed isoprene fluxes are a minimum in May, and only have an exponential temperature dependence [*Guenther et al.*, 2006] during the dry season.

[15] Previous analysis of satellite-derived MODIS Leaf-Area Index (LAI) and Enhanced Vegetation Index (EVI) over the Amazon showed that there is significant leaf flushing during the wet-to-dry transition period [*Myneni et al.*, 2007], suggestive of the vegetation anticipating the light-rich conditions associated with the dry season, followed by a significant greening during the dry season [*Huete et al.*, 2006]. Figure 2 shows the temporal variation of LAI and EVI is remarkably consistent with our observed reduction in HCHO during the wet-to-dry transition period (correlations of 0.69 and 0.67, respectively). The timing of this leaf flushing may be critical for the transition between photosynthetic uptake and respiratory losses of carbon. Young leaves quickly gain the capacity to photosynthesize and take up carbon, but the ability to produce and emit isoprene occurs a few weeks later. Since only about a third of all tree species have the ability to emit isoprene, isoprene emissions would be greatly diminished if all or most isoprene-emitting trees flushed their leaves during the wet-to-dry transition. The light-rich environment of the dry season is also associated with elevated leaf temperatures due to high solar insolation and limitations on the water used for transpirational cooling. Whilst the HCHO columns are negatively correlated with precipitation over the Amazon (Figure S1), the exact role of water stress on isoprene emissions is still unclear owing to the deep rooting of rainforest ecosystems [*Nepstad et al.*, 1994]; increased cloud cover may have a greater effect than water availability.

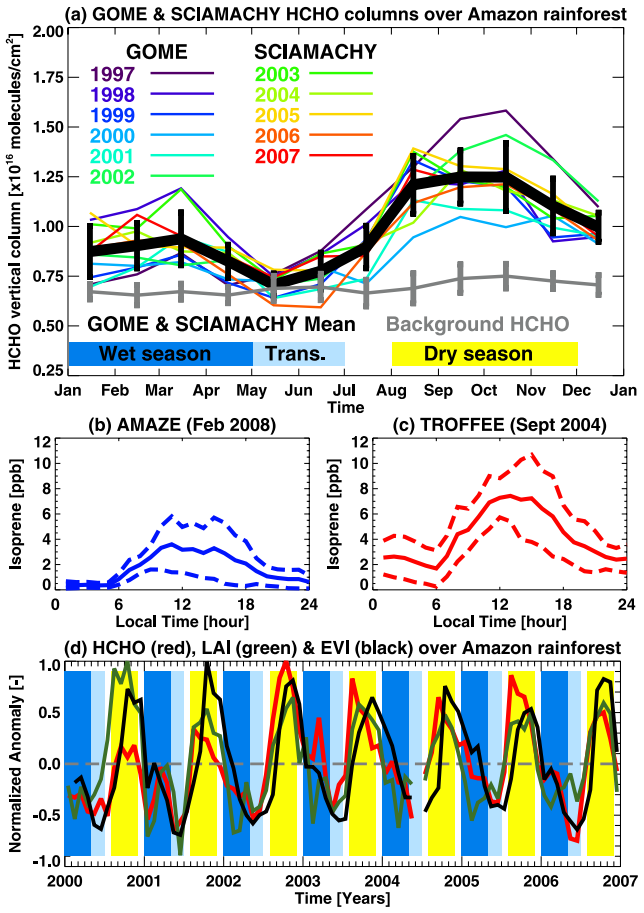

Figure 2. (a) The seasonal cycle of monthly-mean GOME and SCIAMACHY HCHO columns, over the Amazon rainforest (Figure S4) from 1997 to 2007, averaged on a 2° × 2.5° grid using columns with fractional cloud cover ≤40%. Grid squares influenced by surface fires, identified using firecounts and GOME/SCIAMACHY nitrogen dioxide columns, are discarded. The wet, transition, and dry seasons are denoted by dark blue, light blue, and yellow regions, respectively. The simulated HCHO background (for 2000), from the oxidation of non-isoprene species is shown in grey (see auxiliary material). Isoprene concentrations measured in a primary forest reserve (2.5°S, 60.2°W) during (b) the AMazonian Aerosol characteriZation Experiment (AMAZE), February–March, 2008 (T. Karl, Biosphere atmosphere exchange of VOC, NO_x and O_3 in Amazonia during the wet season, manuscript in preparation, 2008) and during (c) the TROpical Forest and Fire Emission Experiment (TROFFEE), August–September, 2004 [*Karl et al.*, 2007]. The solid lines denote the mean values over the experiments, and the dashed lines denote the one standard deviation about that mean. (d) Normalized anomalies of GOME/SCIAMACHY HCHO columns and MODIS Leaf-Area Index (LAI) and Enhanced Vegetation Index (EVI) over the Amazon rainforest from 2000 to 2006.

[16] Our results suggest that isoprene emitters experience large-scale leaf flushing prior to the dry season. This leaf flushing, which is likely caused by an anticipatory response to seasonal changes in solar radiation [*Myneni et al.*, 2007], appears to trigger a significant decrease in regional isoprene emissions. The implications of our results for the oxidizing capacity of the Tropics during the wet-to-dry transition period are also unclear due to uncertain isoprene chemistry, particularly under conditions with low nitrogen oxide concentrations.

5. Outlook

[17] The HCHO, LAI and EVI data are currently the only independent long-term measurements of terrestrial biogenic activity on continental scales and their remarkable consistency provides considerable confidence. There are clearly major gaps in our current understanding of the leaf phenology, biochemistry and atmospheric chemistry of isoprene, particularly over the Tropics that must be addressed either by long-term flux and concentration measurements or by measurement campaigns that target the wet-to-dry period to improve understanding of the relationships between biology, phenology, hydrology, and meteorological drivers.

[18] **Acknowledgments.** This work was supported by the National Environment Research Council (grants NE/D001471 and RG CHEM 461400). We thank Randall Martin for providing GOME/SCIAMACHY NO_2 data and the ESA portal for the ATSR firecounts.

References

Arneth, A., R. K. Monson, G. Schurgers, U. Niinemets, and P. I. Palmer (2008), Why are estimates of global terrestrial isoprene emissions so similar (and why is this not so for monoterpenes)?, *Atmos. Chem. Phys.*, *8*, 4605–4620.

Barkley, M. P., P. I. Palmer, U. Kuhn, J. Kesselmeier, K. Chance, T. P. Kurosu, R. V. Martin, D. Helmig, and A. Guenther (2008), Net ecosystem fluxes of isoprene over tropical South America inferred from GOME observations of HCHO columns, *J. Geophys. Res.*, *113*, D20304, doi:10.1029/2008JD009863.

Bovensmann, H., J. P. Burrows, M. Buchwitz, J. Frerick, S. Nöel, V. V. Rozanov, K. V. Chance, and A. Goede (1999), SCIAMACHY: Mission objectives and measurement modes, *J. Atmos. Sci.*, *56*, 127–150.

Burrows, J. P., et al. (1999), The Global Ozone Monitoring Experiment (GOME): Mission concept and first scientific results, *J. Atmos. Sci.*, *56*, 151–175.

Chance, K., P. I. Palmer, R. J. D. Spurr, R. V. Martin, T. P. Kurosu, and D. J. Jacob (2000), Satellite observations of formaldehyde over North America from GOME, *Geophys. Res. Lett.*, *27*(21), 3461–3464, doi:10.1029/2000GL011857.

Claeys, M., et al. (2004), Formation of secondary organic aerosols through photooxidation of isoprene, *Science*, *303*, 1173–1176, doi:10.1126/science.1092805.

De Smedt, I., J.-F. Müller, T. Stavrakou, R. van der A, H. Eskes, and M. V. Roozendael (2008), Twelve years of global observation of formaldehyde in the troposphere using GOME and SCIAMACHY sensors, *Atmos. Chem. Phys. Discuss.*, *8*, 7555–7608.

Fu, T.-M., D. J. Jacob, P. I. Palmer, K. Chance, Y. X. Wang, B. Barletta, D. R. Blake, J. C. Stanton, and M. J. Pilling (2007), Space-based formaldehyde measurements as constraints on volatile organic compound emissions in east and south Asia and implications for ozone, *J. Geophys. Res.*, *112*, D06312, doi:10.1029/2006JD007853.

Guenther, A., T. Karl, P. Harley, C. Wiedinmyer, P. I. Palmer, and C. Geron (2006), Estimates of global terrestrial isoprene emissions using MEGAN (Model of Emissions of Gases and Aerosols from Nature), *Atmos. Chem. Phys.*, *6*, 3181–3210.

Huete, A. R., K. Didan, Y. E. Shimabukuro, P. Ratana, S. R. Saleska, L. R. Hutyra, W. Yang, R. R. Nemani, and R. Myneni (2006), Amazon rainforests green-up with sunlight in dry season, *Geophys. Res. Lett.*, *33*, L06405, doi:10.1029/2005GL025583.

Karl, T., A. Guenther, R. J. Yokelson, J. Greenberg, M. Potosnak, D. R. Blake, and P. Artaxo (2007), The tropical forest and fire emissions experiment: Emission, chemistry, and transport of biogenic volatile organic compounds in the lower atmosphere over Amazonia, *J. Geophys. Res.*, *112*, D18302, doi:10.1029/2007JD008539.

Kesselmeier, J., et al. (2002), Concentrations and species composition of atmospheric volatile organic compounds (VOCs) as observed during the wet and dry season in Rondnia (Amazonia), *J. Geophys. Res.*, *107*(D20), 8053, doi:10.1029/2000JD000267.

Koelemeijer, R. B. A., P. Stammes, J. W. Hovenier, and J. F. de Haan (2002), Global distributions of effective cloud fraction and cloud top pressure derived from oxygen A band spectra measured by the Global Ozone Monitoring Experiment: Comparison to ISCCP data, *J. Geophys. Res.*, *107*(D12), 4151, doi:10.1029/2001JD000840.

Kylling, K., P. Stamnes, and S.-C. Tsay (1995), A reliable and efficient two-stream algorithm for spherical radiative transfer: Documentation of accuracy in realistic layered media, *J. Atmos. Phys.*, *21*, 115–150.

Malhi, Y., and J. Wright (2004), Spatial patterns and recent trends in the climate of tropical forest regions, *Philos. Trans. R. Soc., Part A*, *359*, 311–329.

Martin, R. V., et al. (2002), An improved retrieval of tropospheric nitrogen dioxide from GOME, *J. Geophys. Res.*, *107*(D20), 4437, doi:10.1029/2001JD001027.

Müller, J.-F., and T. Stavrakou (2005), Inversion of CO and NO_x emissions using the adjoint of the IMAGES model, *Atmos. Chem. Phys.*, *5*, 1157–1186.

Müller, J.-F., et al. (2008), Global isoprene emissions estimated using MEGAN, ECMWF analyses and a detailed canopy environment model, *Atmos. Chem. Phys.*, *8*, 1329–1341.

Myneni, R. B., et al. (2007), Large seasonal swings in leaf area of Amazon rainforests, *Proc. Natl. Acad. Sci.*, *104*, 4820–4823, doi:10.1073/pnas.0611338104.

Nepstad, D. C., C. R. de Carvalho, E. A. Davidson, P. Jipp, P. Lefebvre, G. H. Negreiros, E. D. da Silva, S. T. T. Stone, and S. Vieira (1994), The role of deep roots in the hydrological and carbon cycles of Amazonian forests and pastures, *Nature*, *372*, 666–669, doi:10.1038/372666a0.

Palmer, P. I., D. J. Jacob, K. Chance, R. V. Martin, R. J. D. Spurr, T. P. Kurosu, I. Bey, R. Yantosca, A. Fiore, and Q. Li (2001), Air mass factor formulation for spectroscopic measurements from satellites: Application to formaldehyde retrievals from the Global Ozone Monitoring Experiment, *J. Geophys. Res.*, *106*, 14,539–14,550.

Palmer, P. I., D. J. Jacob, A. M. Fiore, R. V. Martin, K. Chance, and T. P. Kurosu (2003), Mapping isoprene emissions over North America using formaldehyde column observations from space, *J. Geophys. Res.*, *108*(D6), 4180, doi:10.1029/2002JD002153.

Palmer, P. I., et al. (2006), Quantifying the seasonal and interannual variability of North American isoprene emissions using satellite observations of the formaldehyde column, *J. Geophys. Res.*, *111*, D12315, doi:10.1029/2005JD006689.

Richter, A., and T. Wagner (2001), Diffuser plate spectral structures and their influence on GOME slant columns, technical report, Inst. Environ. Phys., Univ. of Bremen, Bremen, Germany.

Sanderson, M. G., C. D. Jones, W. J. Collins, C. E. Johnson, and R. G. Derwent (2003), Effect of climate change on isoprene emissions and surface ozone levels, *Geophys. Res. Lett.*, *30*(18), 1936, doi:10.1029/2003GL017642.

Trostdorf, C. R., L. V. Gatti, A. Yamazaki, M. J. Potosnak, A. Guenther, W. C. Martins, and J. W. Munger (2004), Seasonal cycles of isoprene concentrations in the Amazonian rainforest, *Atmos. Chem. Phys. Discuss.*, *4*, 1291–1310.

M. P. Barkley and P. I. Palmer, School of GeoSciences, University of Edinburgh, Edinburgh EH93JN, UK. (michael.barkley@ed.ac.uk)

I. De Smedt and M. Van Roozendael, Belgian Institute for Space Aeronomy, B-1180 Brussels, Belgium.

A. Guenther and T. Karl, National Center of Atmospheric Research, Boulder, CO 80303, USA.